Warsaw Breakage Syndrome Associated DDX11 Helicase Resolves G-Quadruplex Structures to Support Sister Chromatid Cohesion

Van Schie / Faramarz et al., *Nature Communications* 2020

Supplementary Figures 1-13

Supplementary Table 1

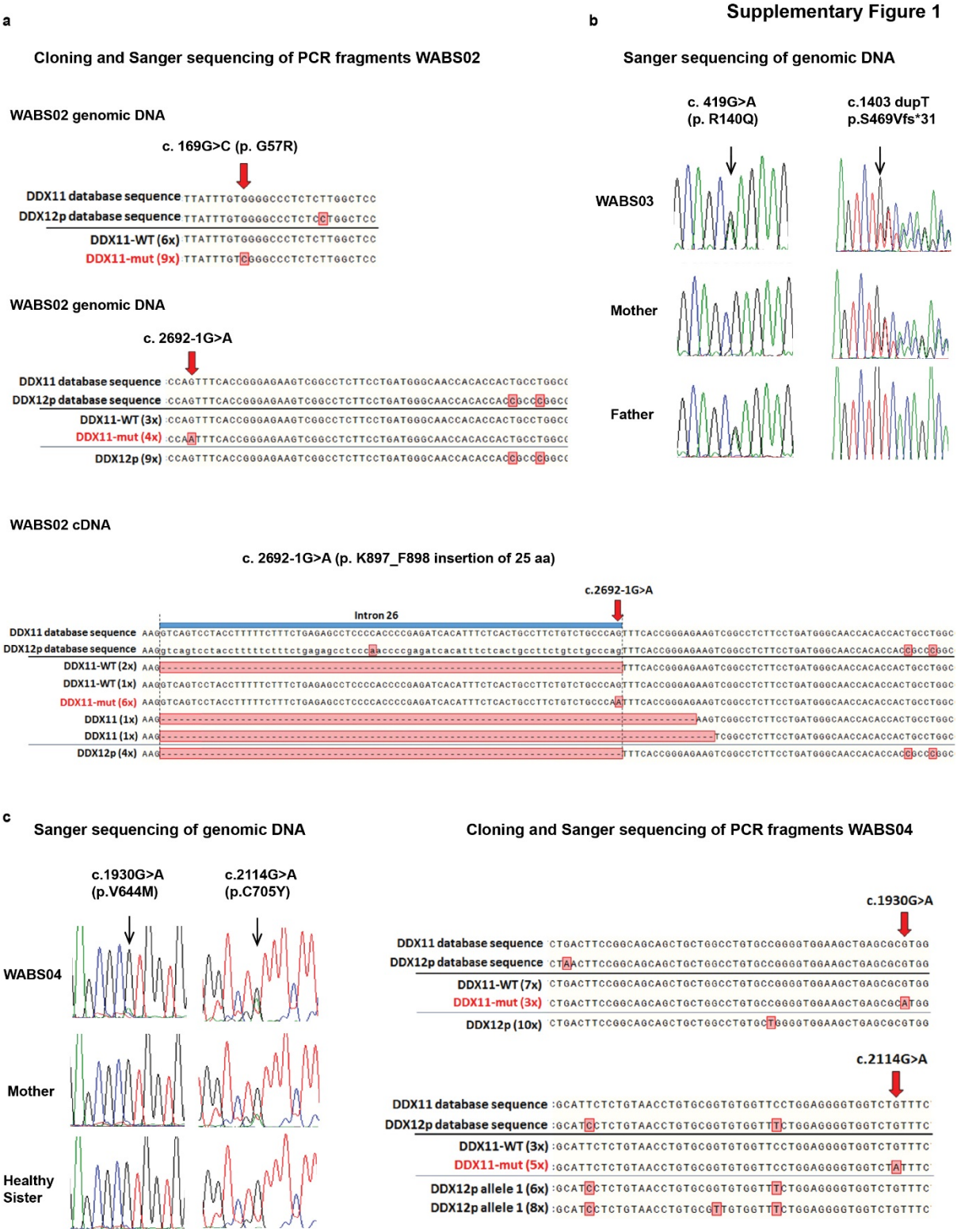
a
Cloning and Sanger sequencing of PCR fragments WABS02
WABS02 genomic DNA
c. 169G>C (p. G57R)
DDX11 database sequence TTATTTGTGGGGCCCTCTCTTGGCTCC
DDX12p database sequence TTATTTGTGGGGCCCTCTCCTGGCTCC
DDX11-WT (6x) TTATTTGTGGGGCCCTCTCTTGGCTCC
DDX11-mut (9x) TTATTTGTCGGGCCCTCTCTTGGCTCC
WABS02 genomic DNA
c. 2692-1G>A
DDX11 database sequence CCAGTTTCACCGGGAGAAGTCGGCCTCTTCCTGATGGGCAACCACACCACTGCCTGGCC
DDX12p database sequence CCAGTTTCACCGGGAGAAGTCGGCCTCTTCCTGATGGGCAACCACACCACCGCCGGCC
DDX11-WT (3x) CCAGTTTCACCGGGAGAAGTCGGCCTCTTCCTGATGGGCAACCACACCACTGCCTGGCC
DDX11-mut (4x) CCAATTTCACCGGGAGAAGTCGGCCTCTTCCTGATGGGCAACCACACCACTGCCTGGCC
DDX12p (9x) CCAGTTTCACCGGGAGAAGTCGGCCTCTTCCTGATGGGCAACCACACCACCGCCGGCC
b
Sanger sequencing of genomic DNA
c. 419G>A
(p. R140Q)
c.1403 dupT
p.S469Vfs*31
WABS03
Mother
Father
WABS02 cDNA
c. 2692-1G>A (p. K897_F898 insertion of 25 aa)
c.2692-1G>A
Intron 26
DDX11 database sequence AAGGTCAGTCCTACCTTTTTCTTTCTGAGAGCCTCCCCACCCCGAGATCACATTTCTCACTGCCTTCTGTCTGCCCAGTTTCACCGGGAGAAGTCGGCCTCTTCCTGATGGGCAACCACACCACTGCCTGGC
DDX12p database sequence AAGgtcagtcctacctttttctttctgagagcctcccaccccgagatcacatttctcactgccttctgtctgcccagTTTCACCGGGAGAAGTCGGCCTCTTCCTGATGGGCAACCACACCACCGCCGGC
DDX11-WT (2x) AAG----------TTTCACCGGGAGAAGTCGGCCTCTTCCTGATGGGCAACCACACCACTGCCTGGC
DDX11-WT (1x) AAGGTCAGTCCTACCTTTTTCTTTCTGAGAGCCTCCCCACCCCGAGATCACATTTCTCACTGCCTTCTGTCTGCCCAGTTTCACCGGGAGAAGTCGGCCTCTTCCTGATGGGCAACCACACCACTGCCTGGC
DDX11-mut (6x) AAGGTCAGTCCTACCTTTTTCTTTCTGAGAGCCTCCCCACCCCGAGATCACATTTCTCACTGCCTTCTGTCTGCCCAATTTCACCGGGAGAAGTCGGCCTCTTCCTGATGGGCAACCACACCACTGCCTGGC
DDX11 (1x) AAG----------AAGTCGGCCTCTTCCTGATGGGCAACCACACCACTGCCTGGC
DDX11 (1x) AAG----------TCGGCCTCTTCCTGATGGGCAACCACACCACTGCCTGGC
DDX12p (4x) AAG----------TTTCACCGGGAGAAGTCGGCCTCTTCCTGATGGGCAACCACACCACCGCCGGC
c
Sanger sequencing of genomic DNA
c.1930G>A
(p.V644M)
c.2114G>A
(p.C705Y)
WABS04
Mother
Healthy
Sister
Cloning and Sanger sequencing of PCR fragments WABS04
c.1930G>A
DDX11 database sequence CTGACTTCCGGCAGCAGCTGCTGGCCTGTGCCGGGGTGGAAGCTGAGCGCGTGG
DDX12p database sequence CTAACTTCCGGCAGCAGCTGCTGGCCTGTGCCGGGGTGGAAGCTGAGCGCGTGG
DDX11-WT (7x) CTGACTTCCGGCAGCAGCTGCTGGCCTGTGCCGGGGTGGAAGCTGAGCGCGTGG
DDX11-mut (3x) CTGACTTCCGGCAGCAGCTGCTGGCCTGTGCCGGGGTGGAAGCTGAGCGCATGG
DDX12p (10x) CTGACTTCCGGCAGCAGCTGCTGGCCTGTGCTGGGGTGGAAGCTGAGCGCGTGG
c.2114G>A
DDX11 database sequence GCATTCTCTGTAACCTGTGCGGTGTGGTTCCTGGAGGGGTGGTCTGTTTC
DDX12p database sequence GCATCCTCTGTAACCTGTGCGGTGTGGTTTCTGGAGGGGTGGTCTGTTTC
DDX11-WT (3x) GCATTCTCTGTAACCTGTGCGGTGTGGTTCCTGGAGGGGTGGTCTGTTTC
DDX11-mut (5x) GCATTCTCTGTAACCTGTGCGGTGTGGTTCCTGGAGGGGTGGTCTATTTC
DDX12p allele 1 (6x) GCATCCTCTGTAACCTGTGCGGTGTGGTTTCTGGAGGGGTGGTCTGTTTC
DDX12p allele 1 (8x) GCATCCTCTGTAACCTGTGCGTTGTGGTTTCTGGAGGGGTGGTCTGTTTC

d

Sanger sequencing of genomic DNA

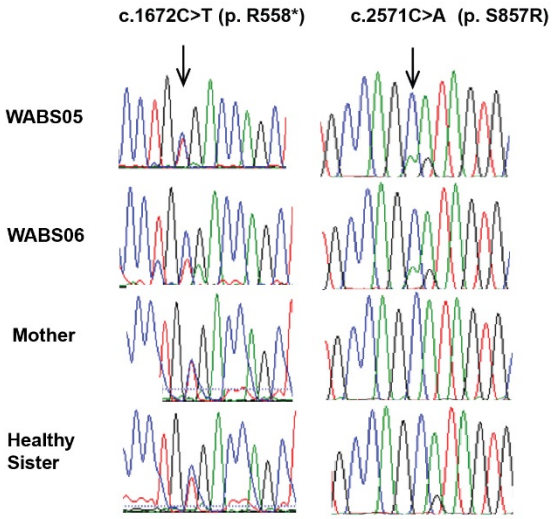

Cloning and Sanger sequencing of PCR fragments WABS05

e

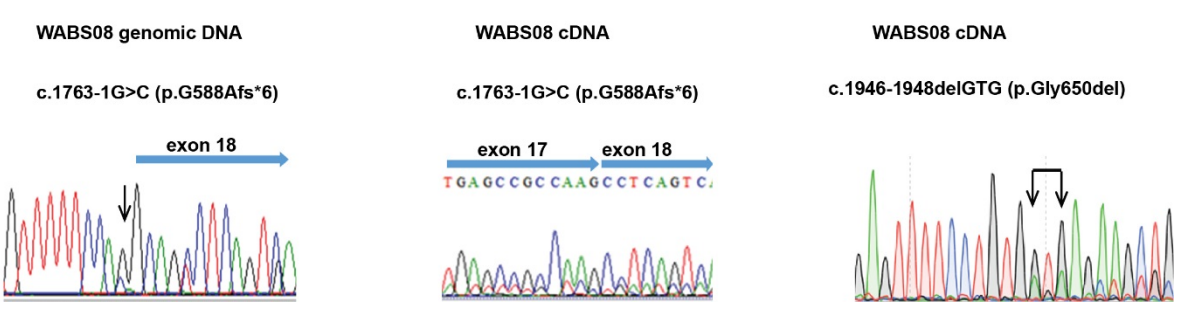

Supplementary Figure 1: Confirmation of pathogenic DDX11 mutations in WABS patients. a) WABS02. PCR fragments, amplified from genomic DNA, were ligated into zero-blunt plasmid, transformed into competent bacteria and DNA from single colonies was sequenced. Sequences were aligned to database DDX11 and DDX12p. One allele contains a c.169G>C missense mutation, leading to a p.G57R substitution. The other allele contains a point mutation affecting the last base of intron 26 (c.2692-1G>A), resulting in retention of intron 26 and in-frame insertion of 25 amino acids at the C-terminus. This was confirmed by sequencing WABS02 cDNA: of seven intron 26 containing reads, six harbored the mutation. b) Sanger sequencing of genomic DNA of WABS03 and both parents. The paternal allele contains a c.419G>A missense mutation, leading to a p.R140Q substitution. The maternal allele contains a c.1403 duplication, leading to a frameshift (p.L468fs*31). c) Sanger sequencing of genomic DNA of WABS04, the mother and a healthy sister. The maternal allele contains a c.2114G>A missense mutation, leading to a p.C705Y substitution. The second allele, not found in the mother and healthy sister, contains a c.1930G>A missense mutation, leading to a p.V644M substitution. To confirm that the mutations are located in DDX11, PCR fragments were ligated into a plasmid and DNA from single colonies was sequenced. Sequences were aligned to database DDX11 and DDX12p. d) Sanger sequencing of genomic DNA of WABS05 and WABS06, the mother and a healthy sister. The maternal allele contains a c.1672C>T nonsense mutation, leading to a premature stop (p.R558*). The second allele contains a c.2571C>A missense mutation, leading to p.S857R substitution. To confirm that mutation c.2571C>A is located in DDX11, PCR fragments were ligated into a plasmid and DNA from single colonies was sequenced. Sequences were aligned to database DDX11 and DDX12p. e, Sanger sequencing of genomic DNA and cDNA of patient WABS08. One allele contains an intronic mutation (c.1763-1G>C) which causes alternative splicing, resulting in deletion of four basepairs in the mRNA and a frameshift (p.G588Afs*6). The second allele contains a splice site mutation, leading to a 3bp deletion in the mRNA (c.1946-1948delGTG) and loss of one amino acid (p.G650del).

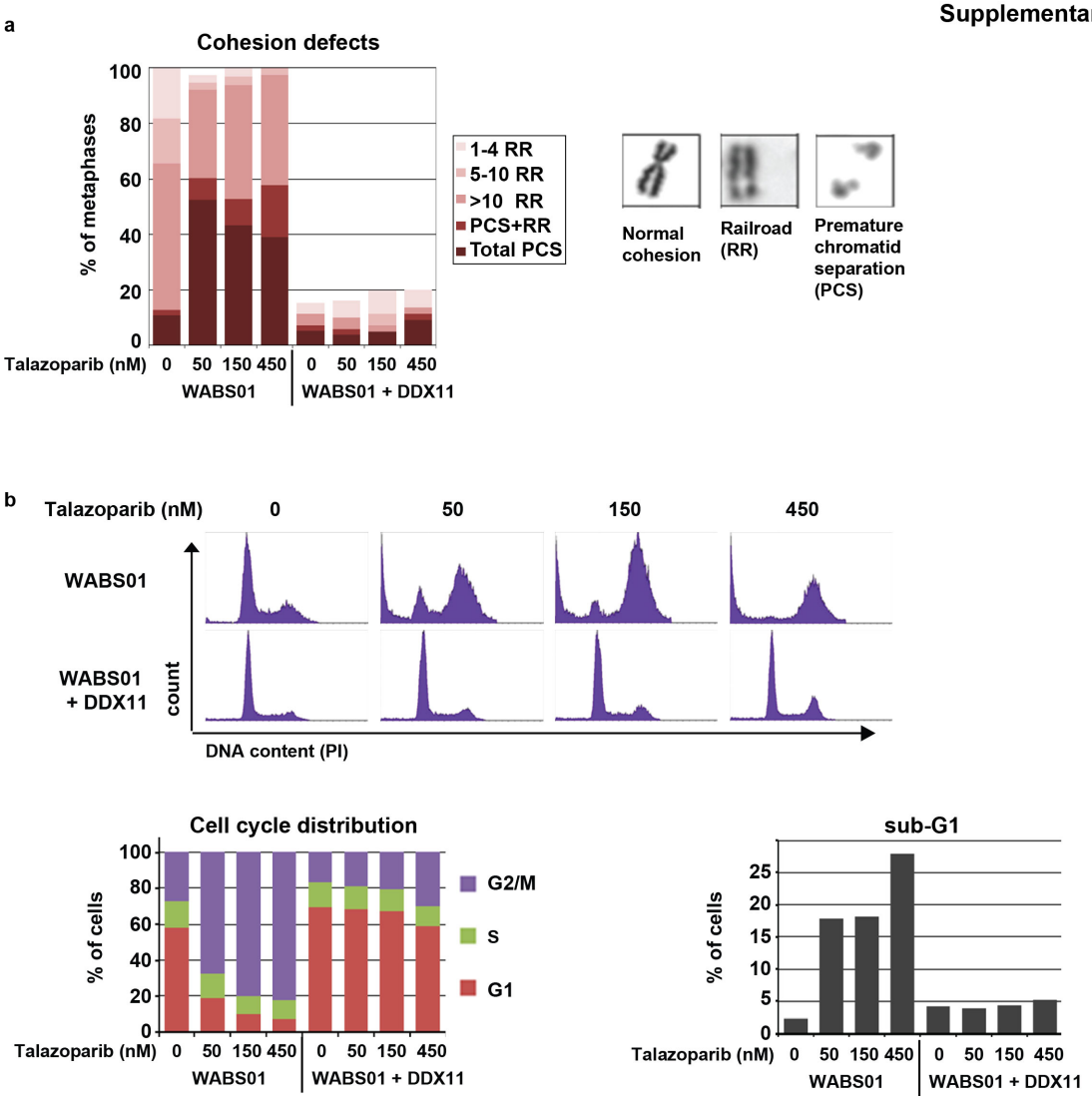

Supplementary Figure 2: Enhanced cohesion loss, G2/M arrest and cell death upon PARPi in WABS fibroblasts. a) cells were treated with indicated doses of talazoparib for 48h and assessed for cohesion defects in 50 metaphases per condition. b) cells were treated with indicated doses of talazoparib for 48h, stained with propidium iodide and analyzed by flow cytometry. Quantifications are shown in the lower graphs.

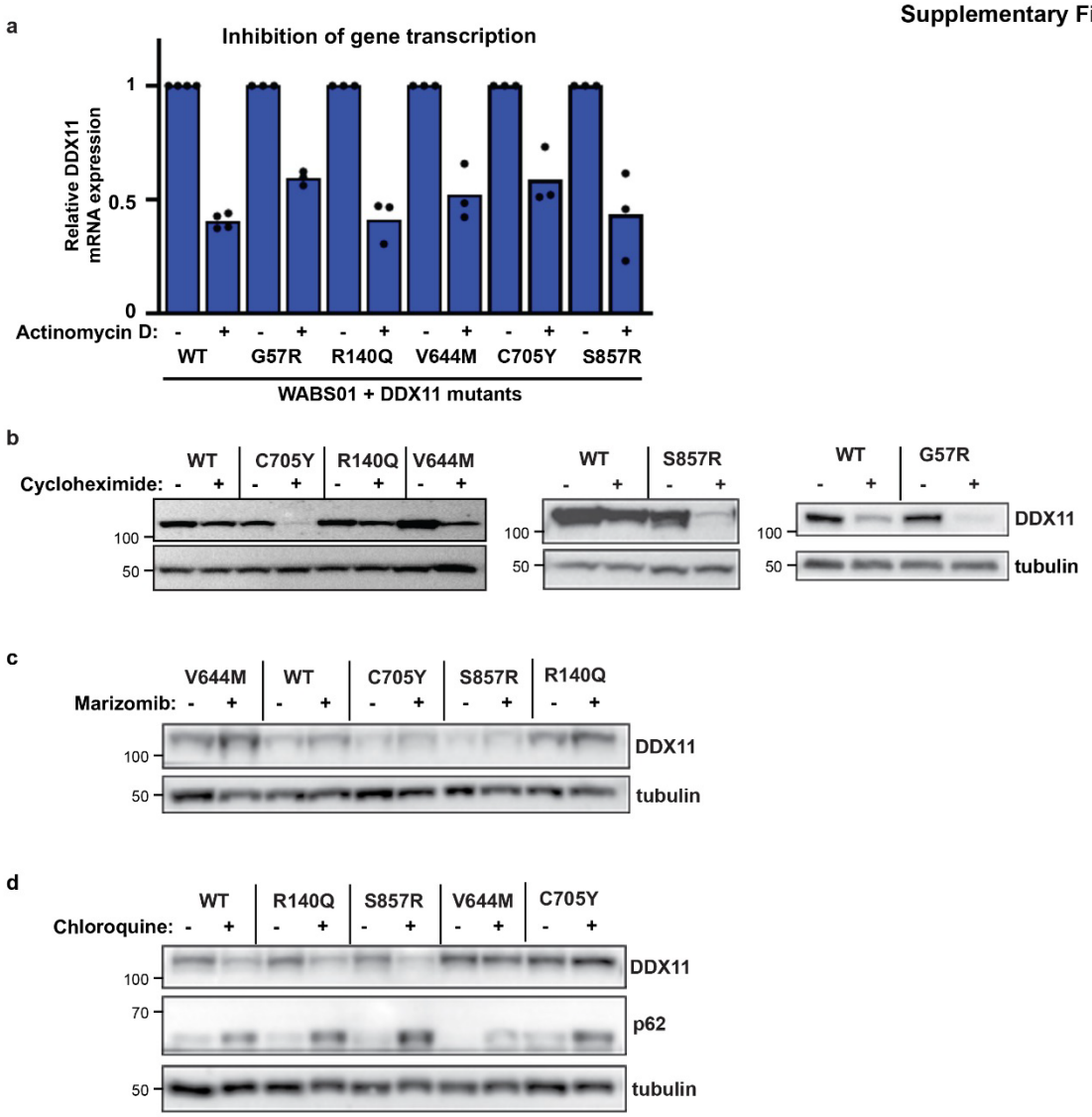

Supplementary Figure 3: DDX11 missense alleles reduce protein stability. a) WABS01 cells, stably transfected with cDNAs encoding either WT-DDX11 or several patient-derived DDX11 mutants, were treated with the transcription inhibitor actinomycin D (5 µg/mL, 4h) and DDX11 mRNA levels were analyzed by qRT-PCR. b-d) Cells were treated with cycloheximide (62,5 µg/mL, 3h), marizomib (500 nM, 5h) or chloroquine (25 µM, 24h). Quantifications from at least two independent experiments are provided in Figure 3e and 3f.

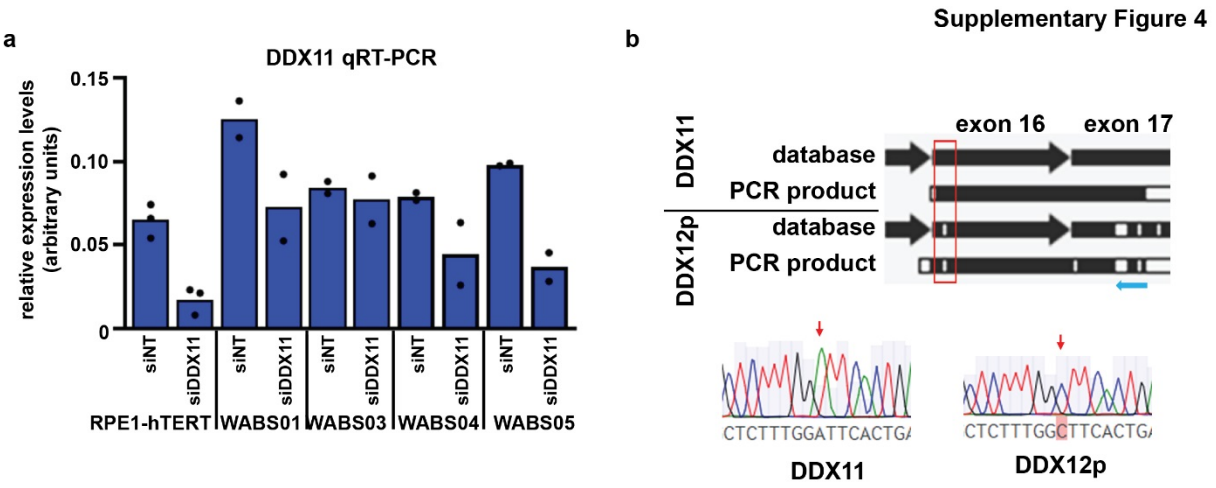

Supplementary Figure 4: Validation of qRT-PCR primers for DDX11 and DDX12p. a) RPE1-hTERT cells and four WABS fibroblasts were transfected with indicated siRNAs (day 1 and day 4) and analyzed for mRNA levels seven days after the first transfection using qRT-PCR. Accompanying cohesion analysis is shown in Figure 3i. b) Specific qRT-PCR primers were designed to distinguish between DDX11 and DDX12p cDNA. This is based on a stretch containing multiple differences in exon 17 (blue arrow). Sanger sequencing of the resulting amplicons confirms specificity of the primers (red arrows).

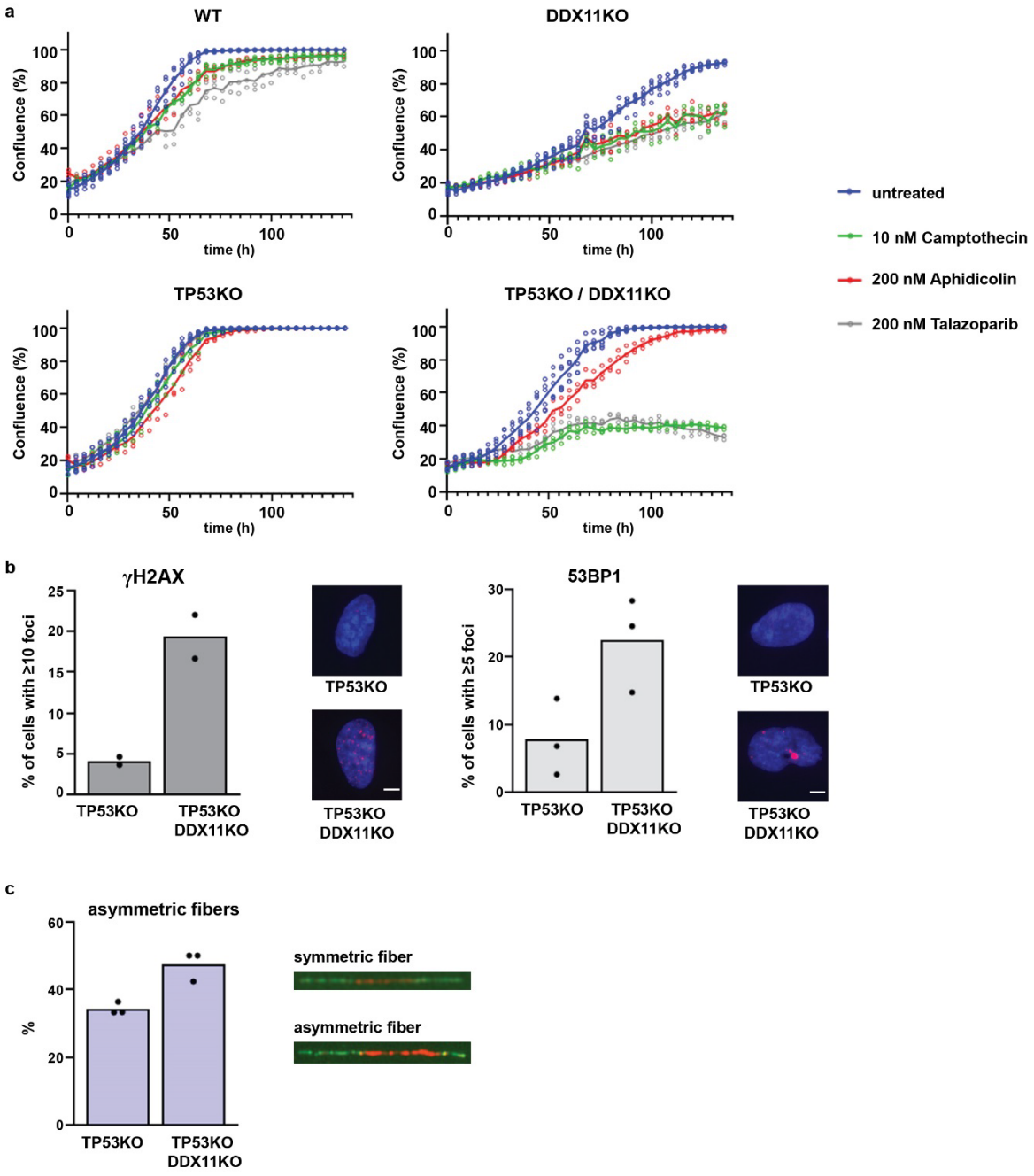

Supplementary Figure 5: Drug sensitivity and basal DNA damage signaling in DDX11 deficient cells. a) RPE1 cells were treated with 10 nM camptothecin, 200 nM aphidicolin or 200 nM talazoparib and growth was monitored using IncuCyte software. Three technical replicates are shown. b) Immunofluorescence detection of γH2AX foci (left) and 53BP1 foci (right) of in total 150 cells per condition in three independent experiments. Scale bar is 5 µm. c) A DNA fiber assay was performed using a double labelling protocol and the percentage of asymmetric forks started from first-label origins as percentage of total first-label-origins is indicated. At least 63 first-label origins were scored in three independent experiments. Representative images of symmetric and asymmetric DNA fibers are shown.

8

Supplementary Figure 6

a

	DDX11		DDX12p	
clone	allele 1	allele 2	allele 1	allele 2
wt-TP53_DDX11/12pKO #13	-13	-13	-8	-9
TP53KO_DDX11/12pKO #6	-11	-13	-10	-11
TP53KO_DDX11/12pKO #7	-2	+1	-8	+5
TP53KO_DDX11KO #1B	+226	?	WT	WT
TP53KO_DDX11KO #8A	-258	?	WT	WT
TP53KO_DDX12pKO #C9	WT	+1	+1	+1
TP53KO_DDX12pKO #C14	WT	+1	+1	+1

b

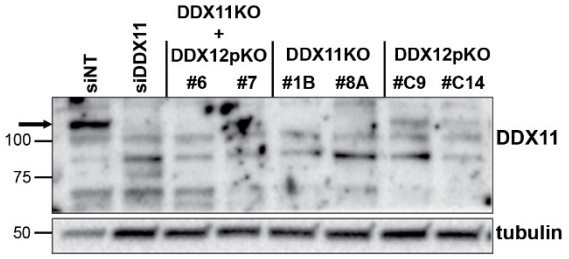

c

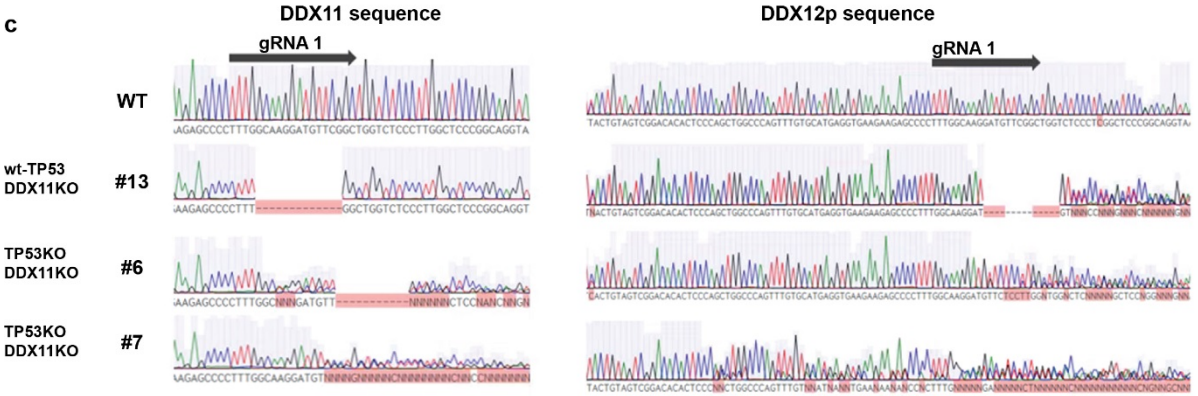

d

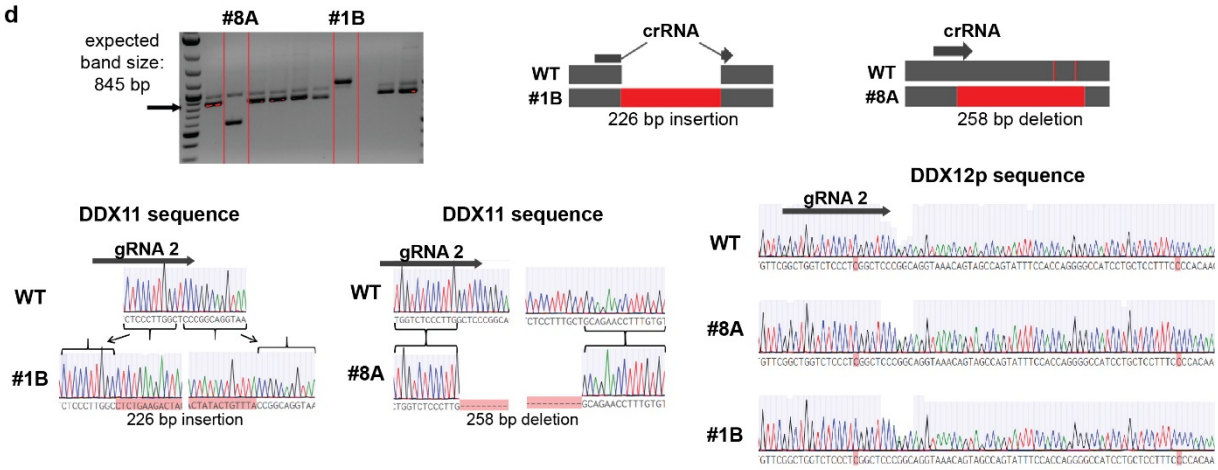

e

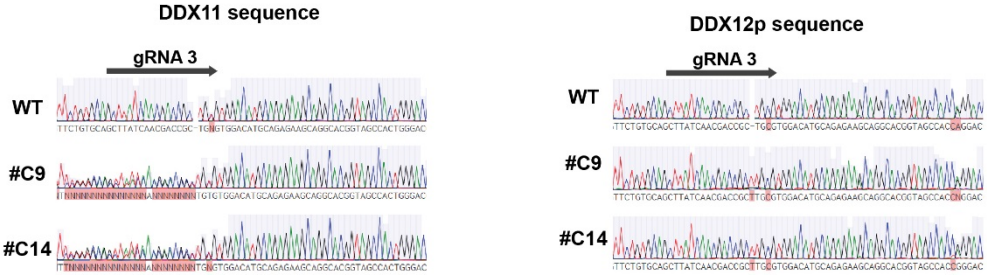

9

Supplementary Figure 6: Characterization of CRISPR-induced indels in DDX11 and DDX12p. a) Summary of indels present in DDX11 and DDX12p knockout clones. RPE1-hTERT_TetOn-Cas9 cells were treated with 100 ng/mL doxycycline to induce Cas9 expression, transfected with synthetic crRNA and tracrRNA and seeded in limiting dilution. DNA from single clones was PCR amplified using DDX11 and DDX12p specific primers, sequenced and analyzed by TIDE [1] for bi-allelic frameshift mutations. Clone #13 (TP53wt, DDX11KO) and clone #6 (TP53KO, DDX11KO) are also used in Figures 4, 6 and 8. b) A panel of RPE1-TP53KO cells with indicated knockout of DDX11 and/or DDX12p was analyzed for DDX11 and tubulin protein levels by western blot. A representative of tree independent protein analyses is shown. c) Sanger sequencing of indels in DDX11 and DDX12p, created with gRNA 1, confirms frameshifts in the selected clones. d) Analysis of the indels that were created with gRNA2. As we had previously observed that gRNA 2 preferentially causes in-frame indels, we co-transfected a PCR-amplified Zeocin resistance expression cassette, to facilitate gene disruption by Zeocin selection. PCR products from the resulting clones were first analyzed on an agarose gel (performed once), indicating loss of the wild-type band in clones #1B and #8A. Sanger sequencing and alignment with control sequence revealed a large insertion and deletion, respectively. We are uncertain what happened to the other allele in both clones, but considering the absence of wildtype product, DDX11 knockout was confirmed. DDX12p sequences are still intact. e) Sanger sequencing of indels in DDX11 and DDX12p, created with gRNA 3. Note that gRNA 3 not only targets both DDX12p alleles, but also one DDX11 allele in RPE1 cells.

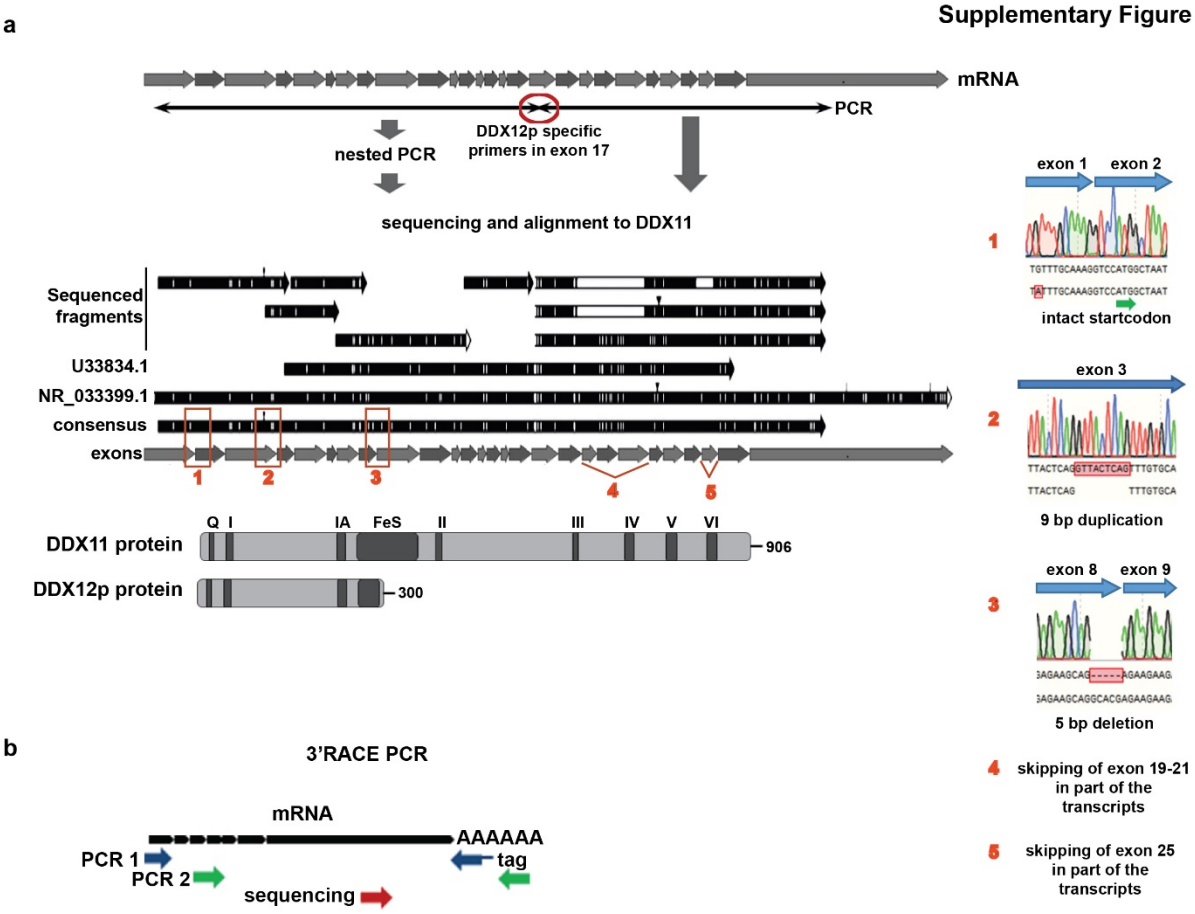
a
mRNA
PCR
DDX12p specific primers in exon 17
nested PCR
sequencing and alignment to DDX11
Sequenced fragments
U33834.1
NR_033399.1
consensus
exons
1
2
3
4
5
Q I
IA
FeS
II
III
IV
V
VI
DDX11 protein
906
DDX12p protein
300
exon 1
exon 2
intact startcodon
exon 3
9 bp duplication
exon 8
exon 9
5 bp deletion
4 skipping of exon 19-21 in part of the transcripts
5 skipping of exon 25 in part of the transcripts
b
3'RACE PCR
mRNA
AAAAAA
PCR 1
PCR 2
tag
sequencing
DDX11 3'end
DDX12p 3'end

Supplementary Figure 7: Identification of the DDX12p mRNA sequences in RPE1 cells. a) DDX12p cDNA was amplified using the DDX12p-specific reverse primers in exon 17 (Supplementary Figure 4). The exon 1-17 amplicon served as template for several subsequent PCR reactions, using primers that do not discriminate between DDX11 and DDX12p. Both the initial exon 17-27 PCR reaction and the nested PCR fragments were ligated into a zero-blunt plasmid, transformed into competent bacteria and DNA of single colonies was sequenced. Sequences were aligned to DDX11 mRNA as well as to the available database mRNA sequence for DDX12p (NR_033399.1 and U3384.1). We find an intact start codon (1) and a 9bp duplication in exon 3 (2). Importantly, the splicing from exon 8 to exon 9 results in a 5bp deletion in the RPE1 DDX12p transcript as compared with database DDX11 and DDX12p sequences (3), resulting in a frameshift and a truncated protein of 300 amino acids. At the 3'end, we find different isoforms that skip exon 19-21 (4) and/or exon 25 (5), but also one that includes all exons. Consensus DDX12p sequence has been deposited to GenBank, and will be available with accession code MT747418. b) 3'RACE PCR confirms a poly-A tail in DDX12p transcripts. RPE1 RNA was reverse transcribed into cDNA using a DDX11/12p forward primer in exon 27 and an oligo-dT reverse primer. A tag on the reverse prime allows a specific 2nd PCR step, and the resulting PCR fragments were ligated into a zero-blunt plasmid, transformed into bacteria and DNA of single colonies was sequenced. Sequences containing multiple base pairs specifically annotated to DDX12p (database sequence, indicated with red arrows) also contain a poly-A tail.

12

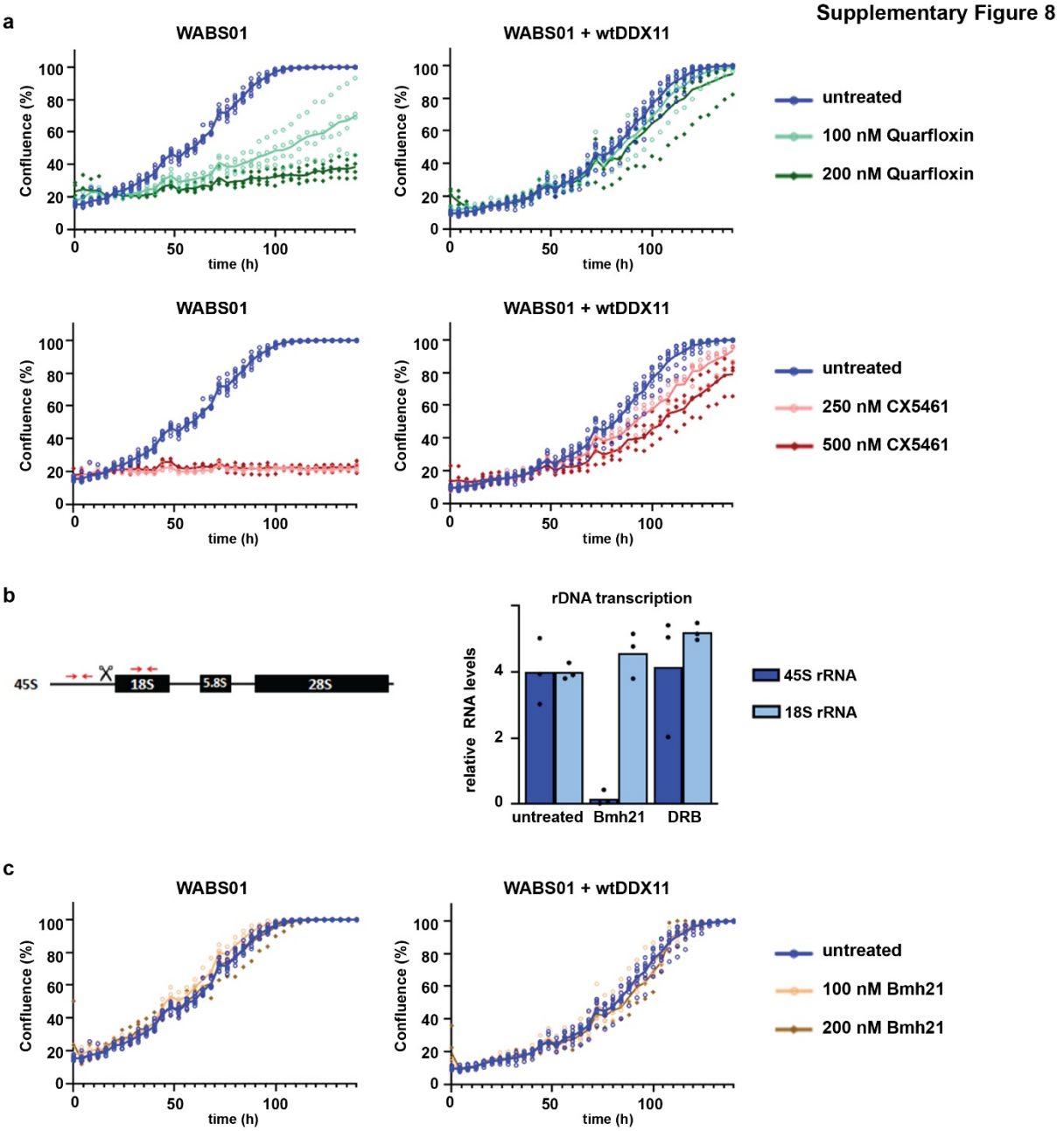

Supplementary Figure 8: DDX11 deficiency sensitizes to G4 stabilization but not to inhibition of rDNA synthesis. a) WABS01 and WABS01 + wtDDX11 fibroblasts were cultured in 96-wells plates and treated with quarfloxin or CX5461. Growth was monitored using IncuCyte software in at least four technical replicates. b) RPE1-hTERT-TP53KO cells were treated with the RNA polymerase II inhibitor DRB or the RNA polymerase I inhibitor Bmh21 (1 µM, 7h) and analyzed by qRT-PCR for ribosomal RNA expression. Red arrows indicate primer locations: the 45S rRNA primer pair amplifies a region that is rapidly cleaved off the large precursor transcript, thereby measuring active rDNA transcription rate. The 18S rRNA primer pair amplifies a highly stable region that is present in mature rRNA, thereby serving as control. c) WABS01 and WABS01 + wtDDX11 fibroblasts were cultured in 96-wells plates and treated with Bmh21. Growth was monitored using IncuCyte software in at least four technical replicates.

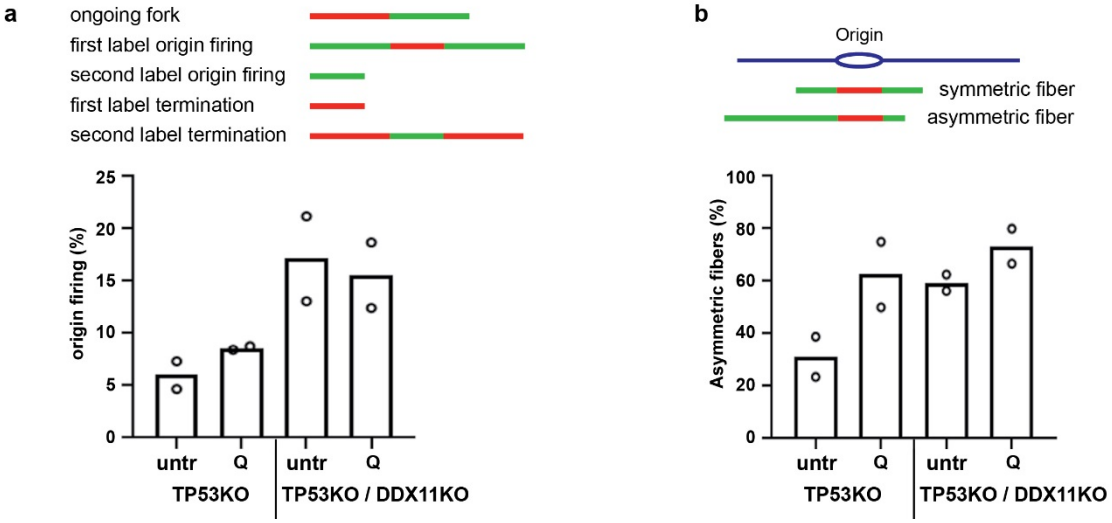

Supplementary Figure 9: Replication fork dynamics upon G4 stabilization and DDX11 depletion. Cells were treated with 200 nM quarfloxin for 24h and assessed with a DNA fiber assay using a double labeling protocol. a) Percentage origin firing was determined for at least 150 fibers in two independent experiments. b) Percentage asymmetric fibers was determined for at least 16 first-label origins in two independent experiments.

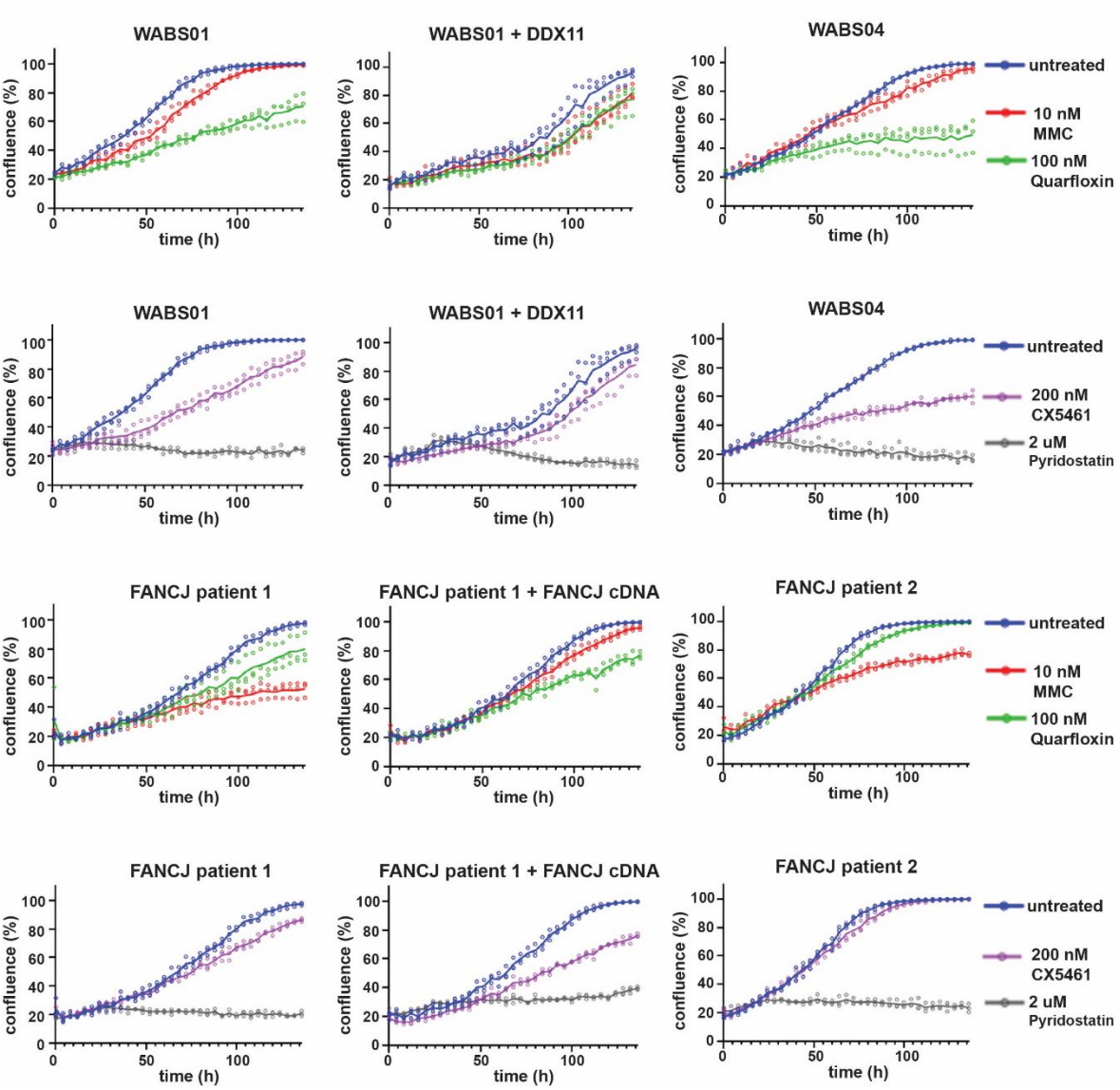

Supplementary Figure 10: Drug sensitivities in WABS cells and FANCJ patient cells. Fibroblasts derived from WABS patients and FANCJ patients were cultured in 96-wells plates and continuously treated as indicated. Growth was monitored using IncuCyte software in three technical replicates.

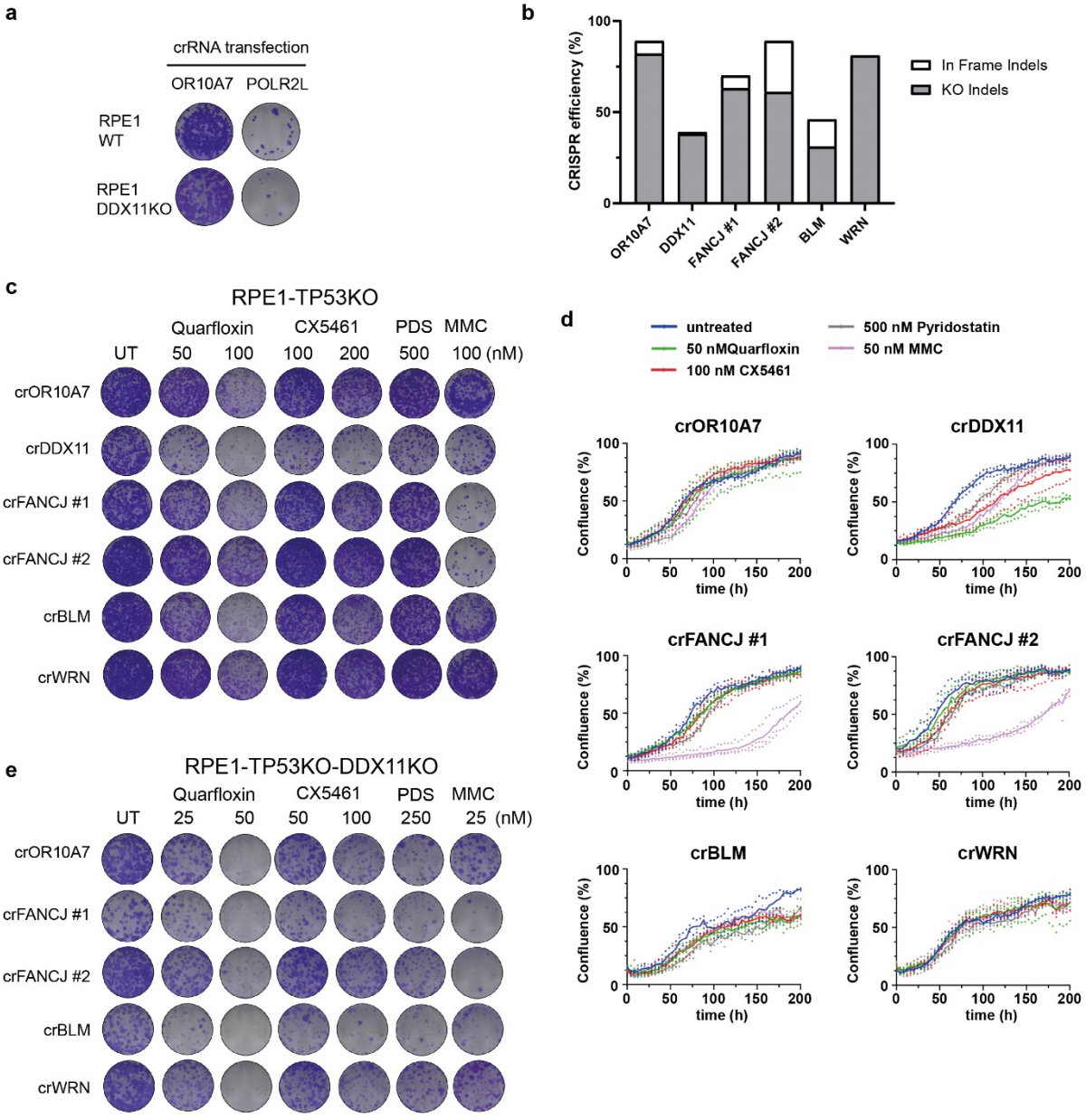

Supplementary Figure 11: Acute gene knockout to assess the role of G4 helicases in G4 stabilizer resistance. a) Clonogenic survival assay was performed of TP53KO and TP53KO-DDX11KO cells two days after Cas9 induction and transfection of synthetic crRNA targeting OR10A7 (negative control) or POLR2L (positive control). b) CRISPR efficiency control by inference of CRISPR edits (ICE) analysis [2]. Percentages of in frame indels and deleterious indels (leading to frameshifts or > 26 bp) at the indicated crRNA target sites are the plotted. c) Clonogenic survival assay of RPE1-TP53KO cells, seeded two days after induction of Cas9 and transfection with indicated crRNAs, treated for 24h as indicated and cultured for another nine days. d) Transfected cells from B were also seeded in 96-wells plates, continuously treated as indicated and growth was monitored using IncuCyte software in three technical replicates. e) RPE1-TP53KO-DDX11KO cells were treated similarly as in b. For all clonogenic survival assays, representative images from two separate experiments are shown.

Supplementary Figure 12

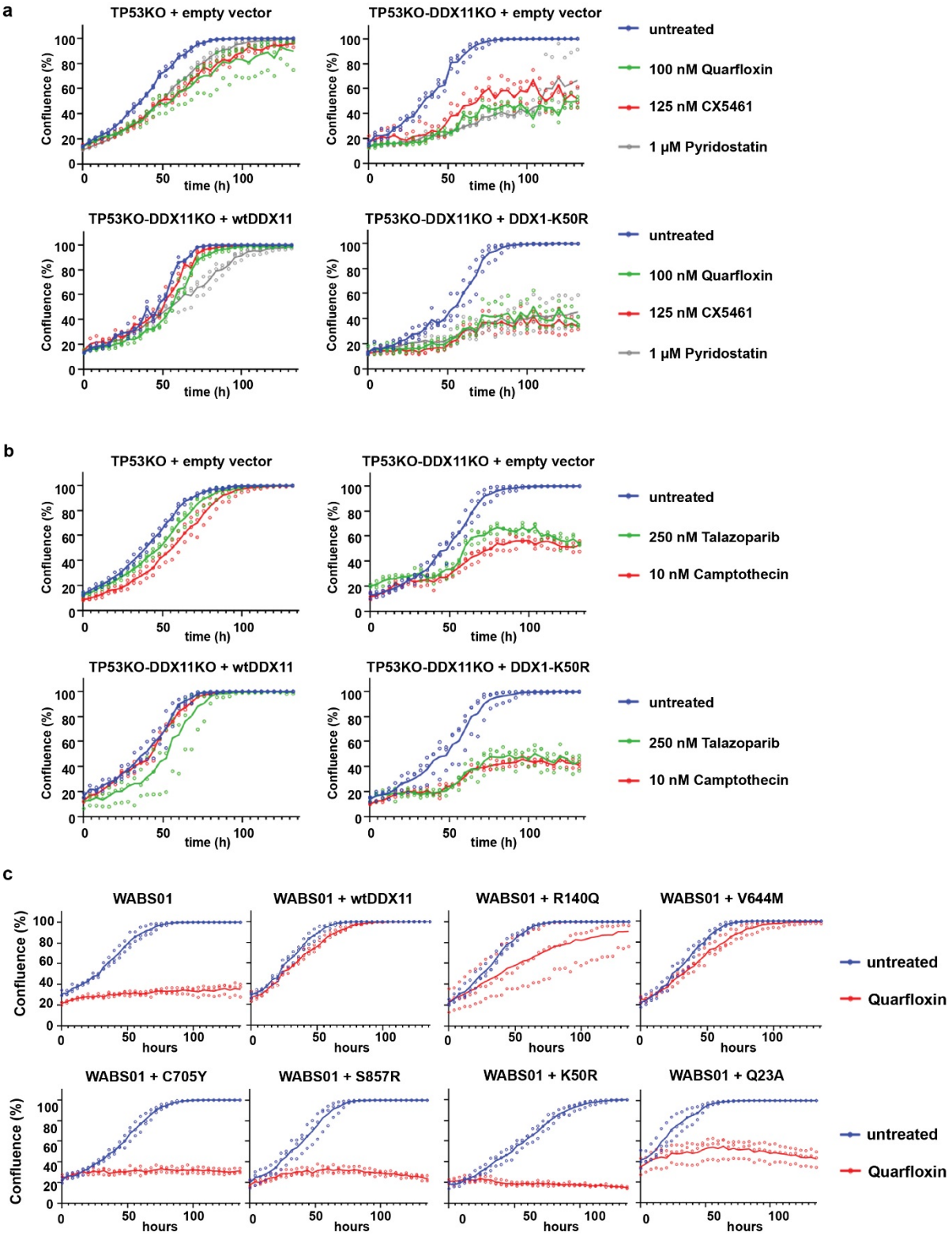

17

Supplementary Figure 12: DDX11 helicase activity is required for resistance to multiple drugs. a) Cells were cultured in 96-wells plates and treated with quarfloxin, CX5461 or pyridostatin. Growth was monitored using IncuCyte software in three technical replicates. b) Similarly, cells were treated with talazoparib or camptothecin and growth was monitored using IncuCyte software. c) Cells were cultured in 96-wells plates and treated with 200 nM quarfloxin. Growth was monitored using IncuCyte software in three technical replicates.

18

Figure 1b

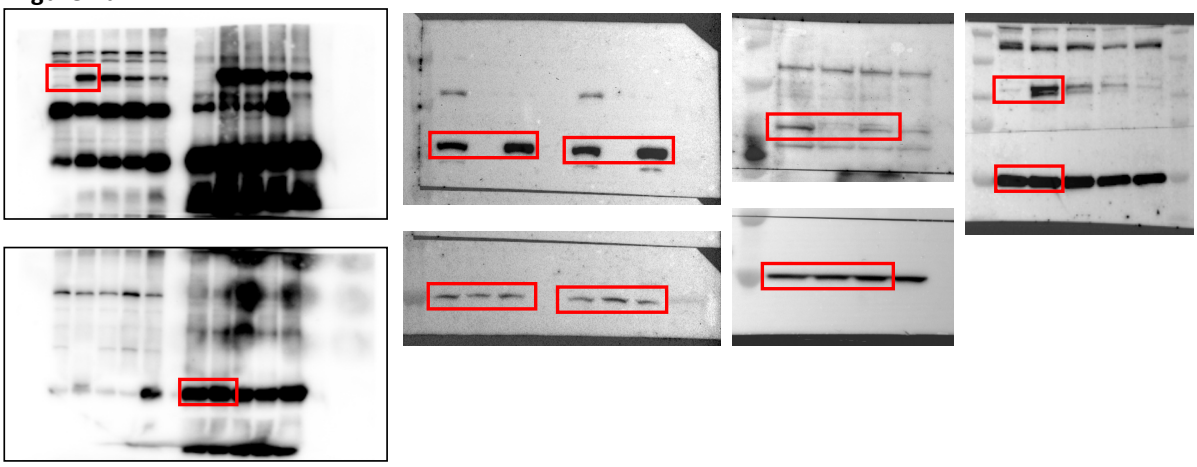

Figure 3a

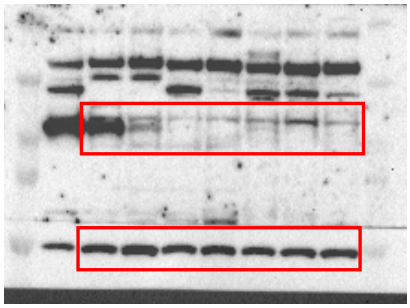

Figure 3c

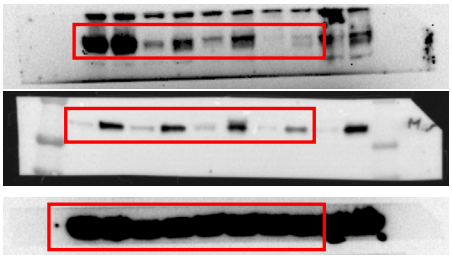

Figure 3d

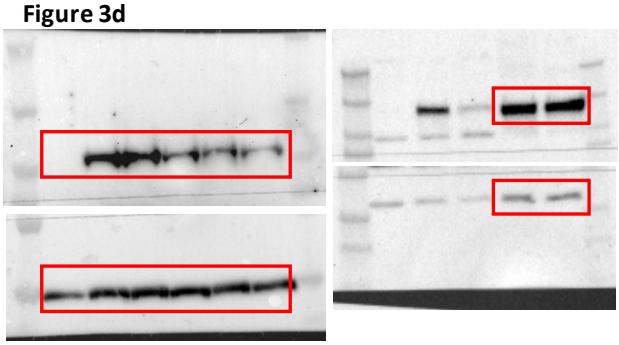

Figure 4b

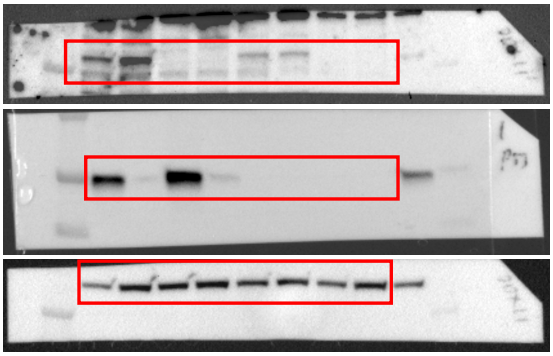

Figure 8a

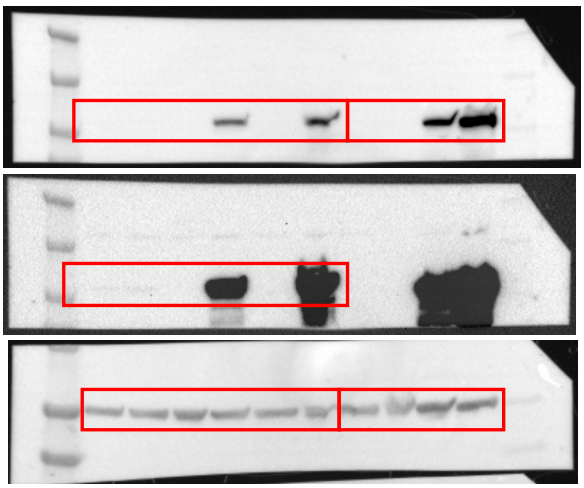

Supplementary Figure 13: uncropped western blots

19

Supplementary Table 1: Primer sequences

Primer name	Sequence
3'RACE 1st PCR Fw	CCAGACAACATCCTGCCCCT
3'RACE 1st PCR Rv #1	TGCCCAGTTCCCAGTTCCGATTTTTTTTTTTTTTTG
3'RACE 1st PCR Rv #2	TGCCCAGTTCCCAGTTCCGATTTTTTTTTTTTTTTC
3'RACE 1st PCR Rv #3	TGCCCAGTTCCCAGTTCCGATTTTTTTTTTTTTTTA
3'RACE 2nd PCR DDX11 Fw	ATTCCAGGTGCATCCAGGCC
3'RACE 2nd PCR DDX12p Fw	TATTCCAGGTGCGGGCGTCA
3'RACE 2nd PCR Rv	TGCCCAGTTCCCAGTTCCGA
3'RACE DDX11 sequencing primer	GGCCCTGCTCCCTATCCTGT
3'RACE DDX12p sequencing primer	GGCCCTGCTCTCTATCCTGC
CRISPR indel sequencing TP53 Fw	GAGACCTGTGGGAAGCGAAA
CRISPR indel sequencing TP53 Rv	GCTGCCCTGGTAGGTTTTCT
CRISPR indel sequencing DDX11 Fw	AACAACCCACCCTCCCCAAG
CRISPR indel sequencing DDX11 Rv	TGCCTCACTCTCTCCAGACC
CRISPR indel sequencing DDX12p Fw	GCTGGGTGGT GCTGGATATG
CRISPR indel sequencing DDX12p Rv	CTGCCTACTGTGGTCTCATCGG
CRISPR indel sequencing OR10A7 Fw	GGATGGCCATAGGCTCTTGGAT
CRISPR indel sequencing OR10A7 Rv	CCTCTTGACAGCCCCTTTCACT
CRISPR indel sequencing FANCJ#1 Fw	GCCACTGTTCTAGGTGCTGTTG
CRISPR indel sequencing FANCJ#1 Rv	CACACCAGAACATAGGCTCCCA
CRISPR indel sequencing FANCJ#2 Fw	GCCTGTGGTACCTTGATCCAGA
CRISPR indel sequencing FANCJ#2 Rv	AGACACATCCTTCGGGGCTATT
CRISPR indel sequencing BLM Fw	tctcagccccaaacgttctgat
CRISPR indel sequencing BLM Rv	ctggtcacaaactcccgacctc
CRISPR indel sequencing WRN Fw	GTGGGATTTGACATGGAGTGGC
CRISPR indel sequencing WRN Rv	ccaggcttaatacccgggtgat
qRT-PCR DDX11 Fw	AACCTGTTCAAGGTGCAGCGATAC
qRT-PCR DDX11 Rv	GAGAAGCTGGTCGCAGGGT
qRT-PCR DDX12p Fw	AACCTGTTCAAGGTGCAGCGATAC
qRT-PCR DDX12p Rv	GGGAAGCTGGTTGCGGGAC
qRT-PCR p21 Fw	AGCAGAGGAAGACCATGTGGA
qRT-PCR p21 Rv	AATCTGTCATGCTGGTCTGCC
qRT-PCR 45S pre-rRNA Fw	GCCTTCTCTAGCGATCTGAGAG
qRT-PCR 45S pre-rRNA Rv	CCATAACGGAGGCAGAGACA
qRT-PCR 18S pre-rRNA Fw	AAACGGCTACCACATCCA
qRT-PCR 18S pre-rRNA Rv	CCTCCAATGGATCCTCGT
qRT-PCR HPRT Fw	TGACACTGGGAAAACAATGCA
qRT-PCR HPRT Rv	GGTCCTTTTCACCAGCAAGCT
qRT-PCR TBP Fw	TGCACAGGAGCCAAGAGTGAA
qRT-PCR TBP Rv	CACATCACAGCTCCCCACCA
qRT-PCR B2M Fw	ATGAGTATGCCTGCCGTGTGA
qRT-PCR B2M Rv	GGCATCTTCAAACCTCCATG
Mouse DDX11 G57R	CTTAAGTCTGATTTGAC
Mouse DDX11 WT	CTTAAGTCTGATTTGTG